Supplementary Materials for

Magnesium regulates the circadian oscillator in cyanobacteria

Young M. Jeong, Cristiano Dias, Casey Diekman, Helene Brochon, Pyonghwa Kim, Manpreet Kaur, Yong-Sung Kim, Hye-In Jang, Yong-Ick Kim*

correspondence to: ykim@njit.edu

This PDF file includes:

Figs. S1 to S14

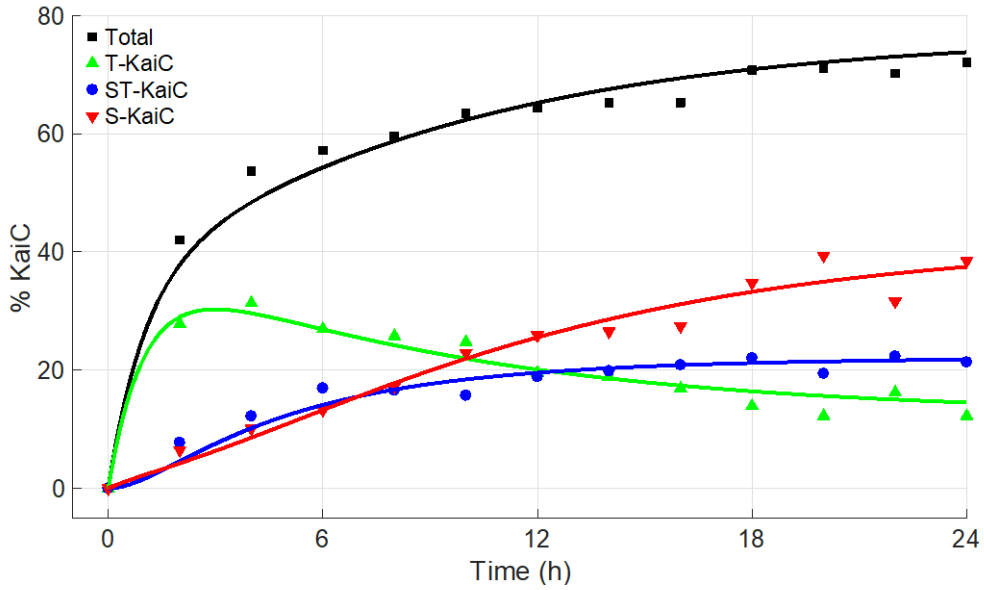

Fig. S1. Mathematical modeling of autonomous phosphorylation of KaiC in the absence of magensium. Experimental data points on the amount of T-KaiC (green triangles), ST-KaiC (blue circles), and S-KaiC (red triangles) were used to fit the model parameters k^B_{XY} representing the baseline transition rates between different phosphoforms in the absence of magnesium. Model simulations with the optimized parameter values are shown for T-KaiC (green curve), ST-KaiC (blue curve), S-KaiC (red curve), and the total amount of phosphorylated KaiC (black curve).

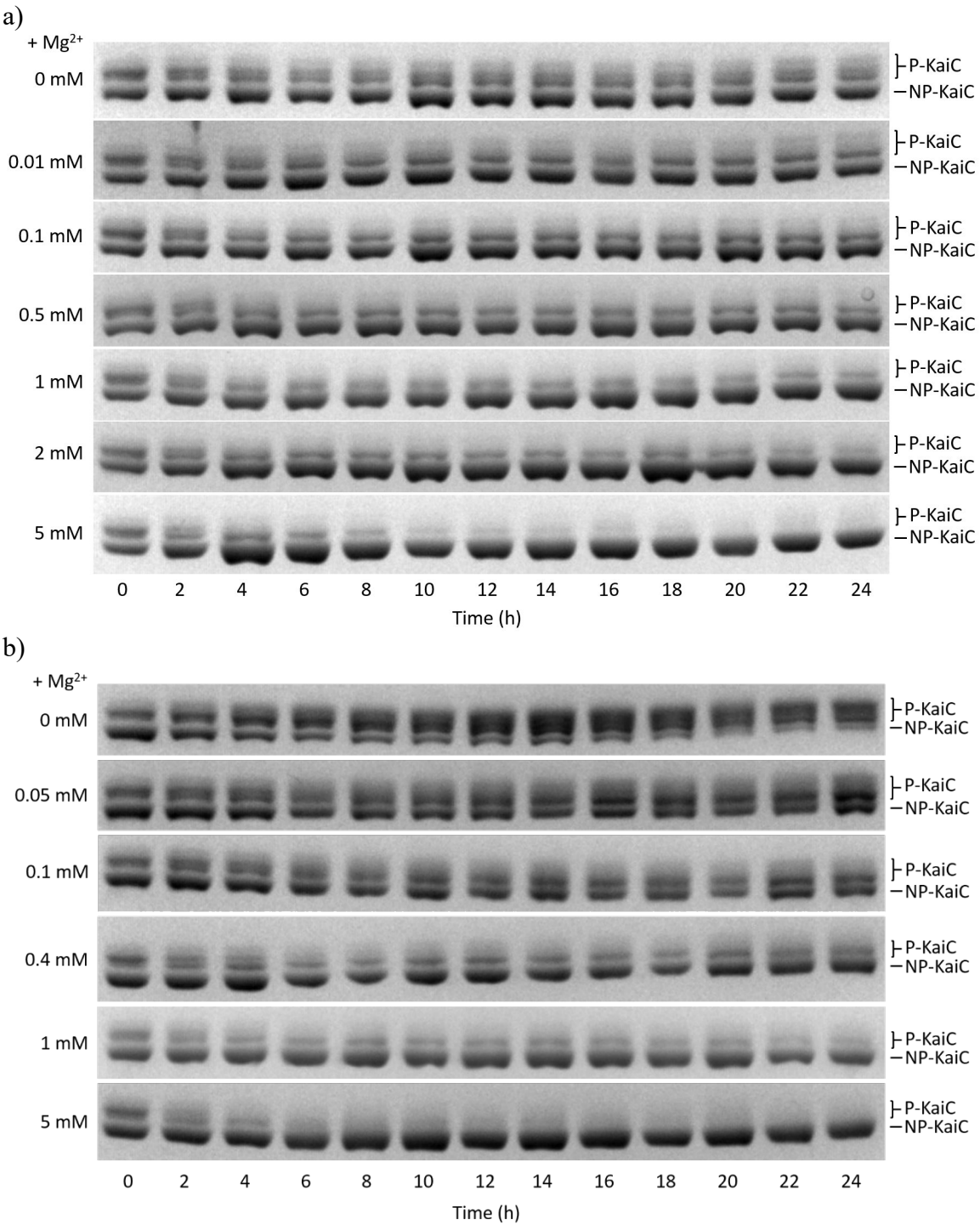

Fig. S2. (**a**) The phosphorylation state of KaiC in the presence of EDTA. The densitometry analysis of the bands is shown in Fig. 1c. (**b**) The phosphorylation state of KaiC in the absence of EDTA. The densitometry analysis of the bands is shown in Fig. 1d**.**

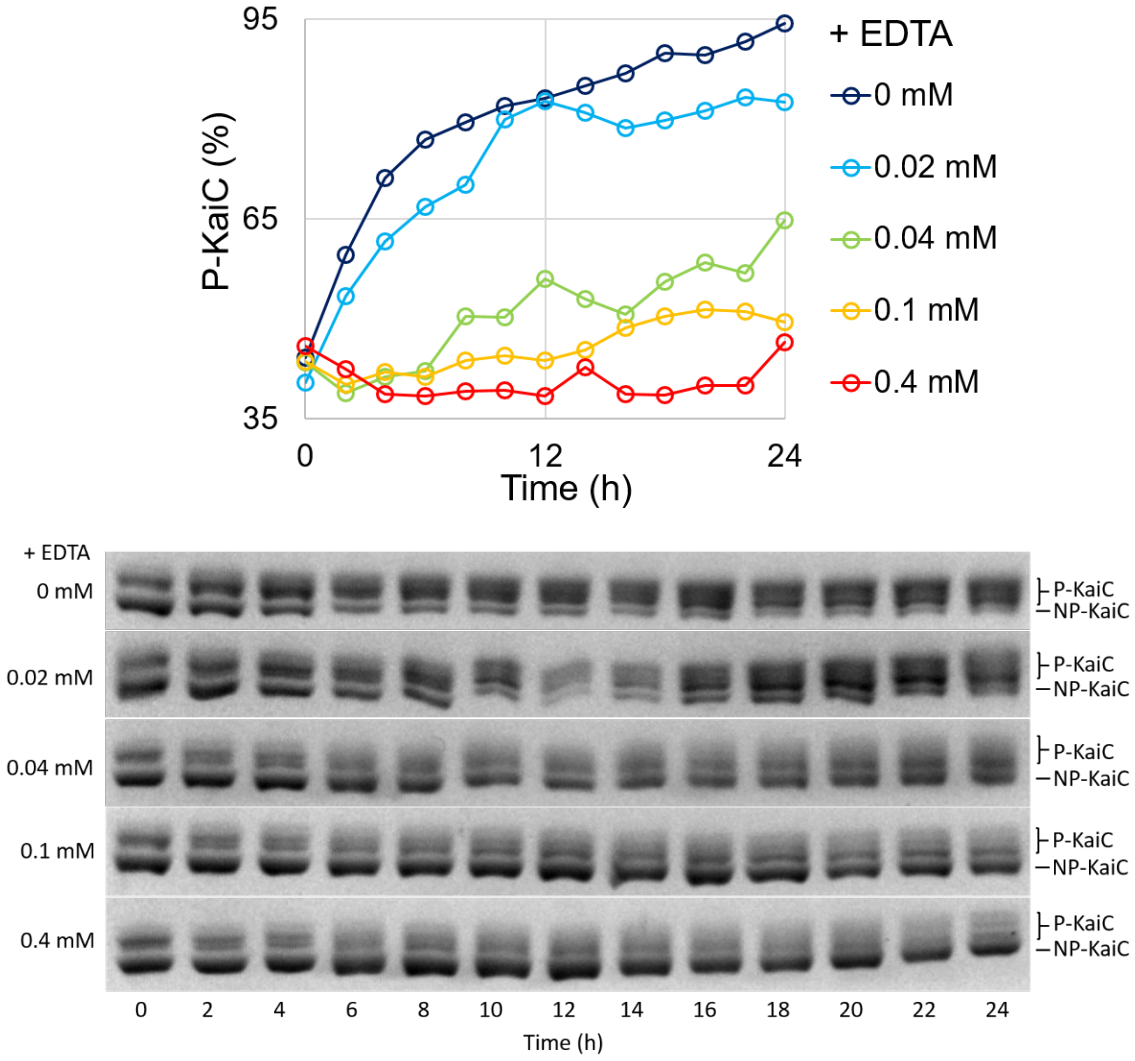

Fig. S3. The phosphorylation state of KaiC in the absence of magnesium.

The densitometry analysis of the bands is shown in upper panel. Phosphorylation state of KaiC in the absence of magnesium with many different EDTA concentrations. EDTA concentrations are labeled on the right of the graph.

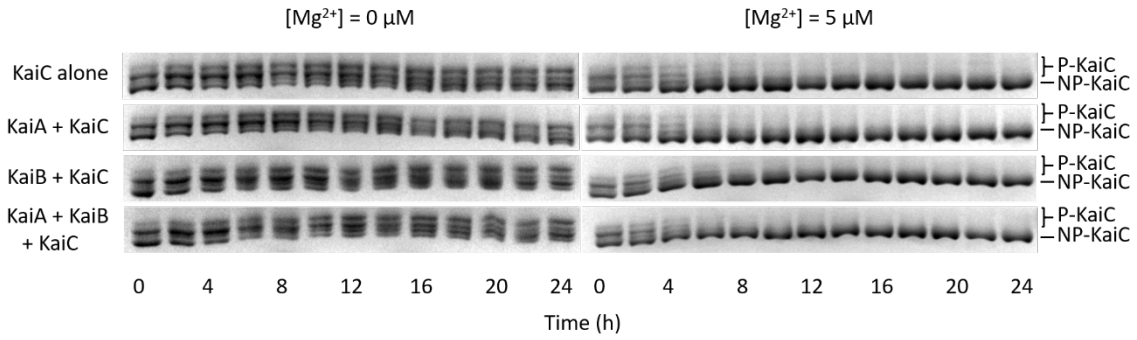

Fig. S4. The phosphorylation state of KaiC497.
The densitometry analysis of the bands is shown in Fig. 1e.

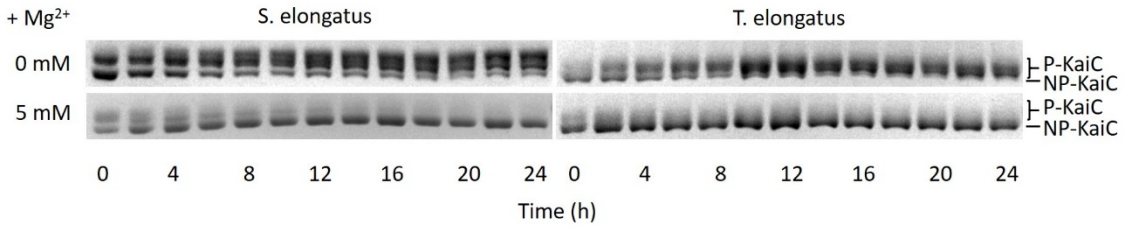

Fig. S5. The phosphorylation state of KaiC from T. elongatus.
The densitometry analysis of the bands is shown in Fig. 1f.

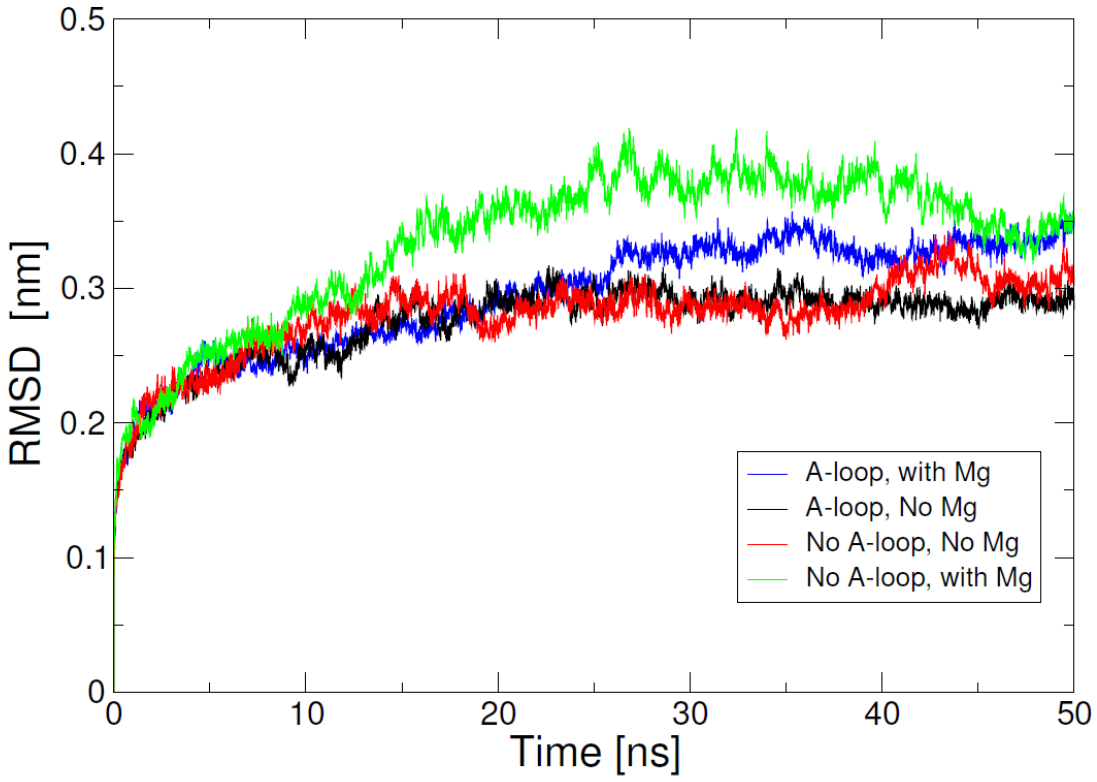

Fig. S6. Root mean square deviation (RMSD) of backbone atoms relative to the initial conformation of the KaiC hexamer.

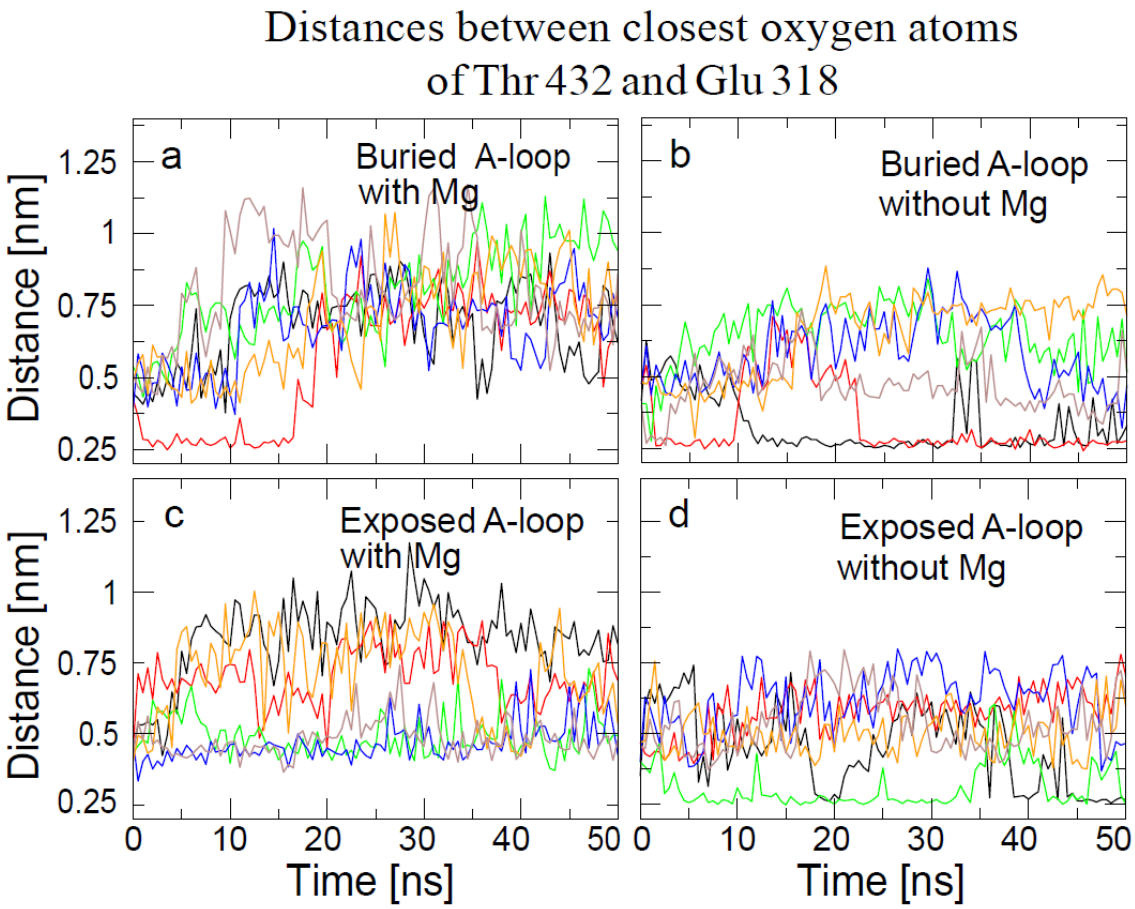

Fig. S7. Distances between closest oxygen atoms of Thr_{432} and Glu_{318} as a function of time.
The A-loop of the KaiC protein is included and deleted from simulations in top (a-b) and bottom (c-d) panels, respectively. Simulations in left (a,c) and right (b,d) panels are performed with and without magnesium, respectively. The six color lines in each panel are the distance result for the six neighboring pairs of T432 and E318 in KaiC hexamer.

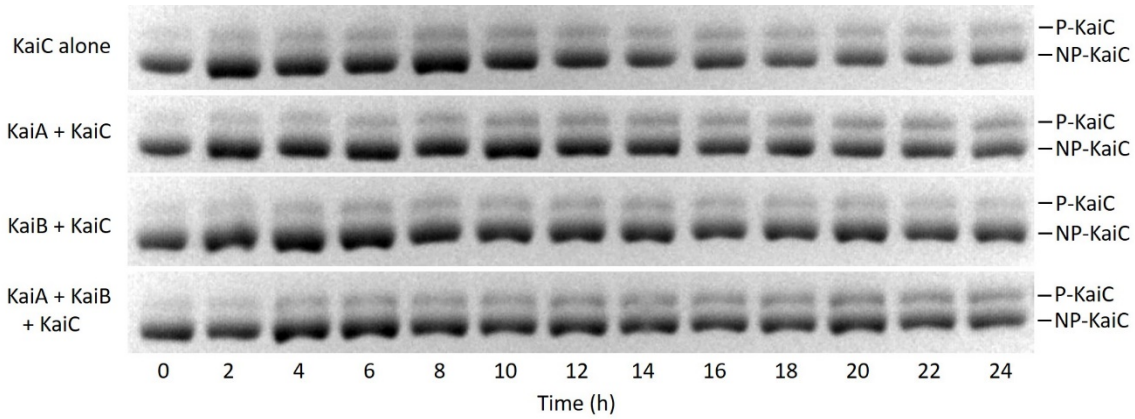

Fig. S8. The phosphorylation state of KaiC E318D.
The densitometry analysis of the bands is shown in Fig. 2d.

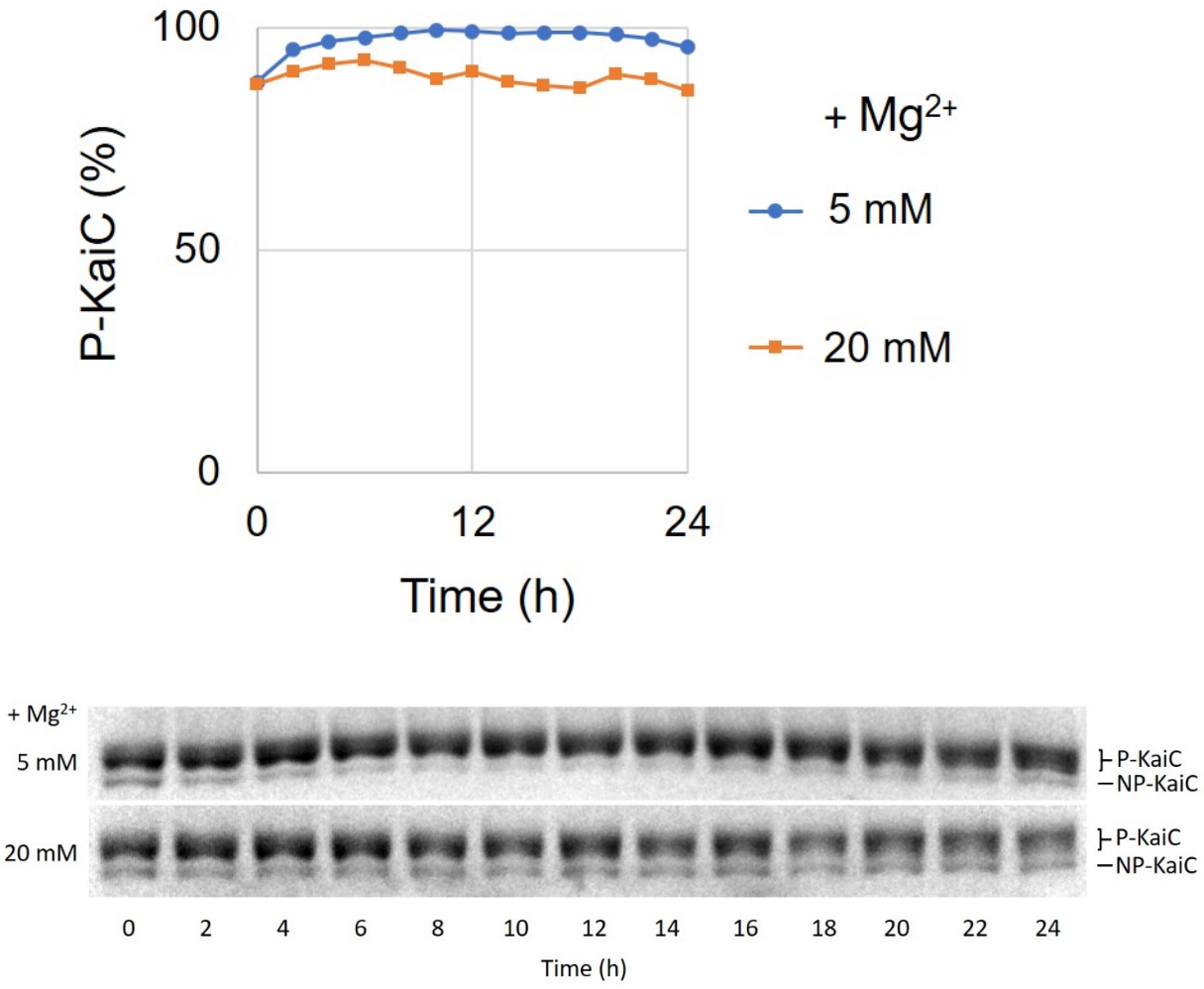

Fig. S9. The phosphorylation state of KaiC E487A in the high magnesium concentration.
The densitometry analysis (upper panel) and SDS-PAGE (bottom panel) of KaiC E487A in 20 mM magnesium concentration

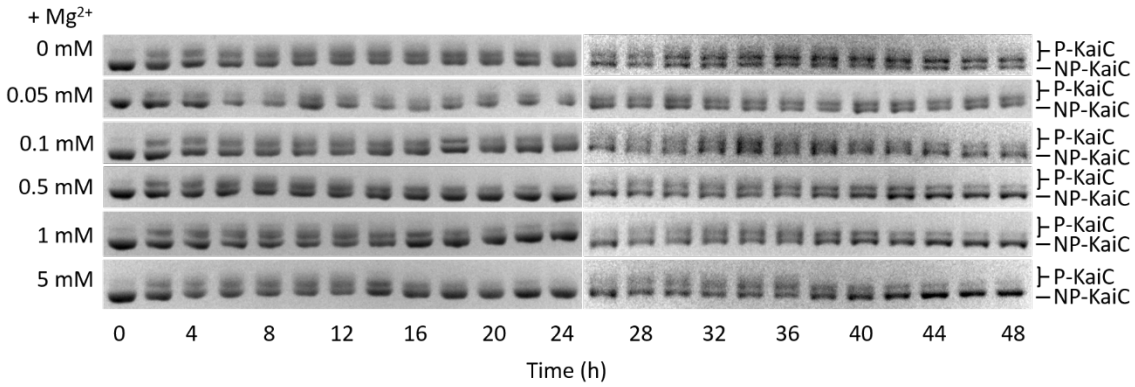

Fig. S10. The phosphorylation state of the hourglass timer of KaiC.
The densitometry analysis of the bands is shown in Fig. 4a.

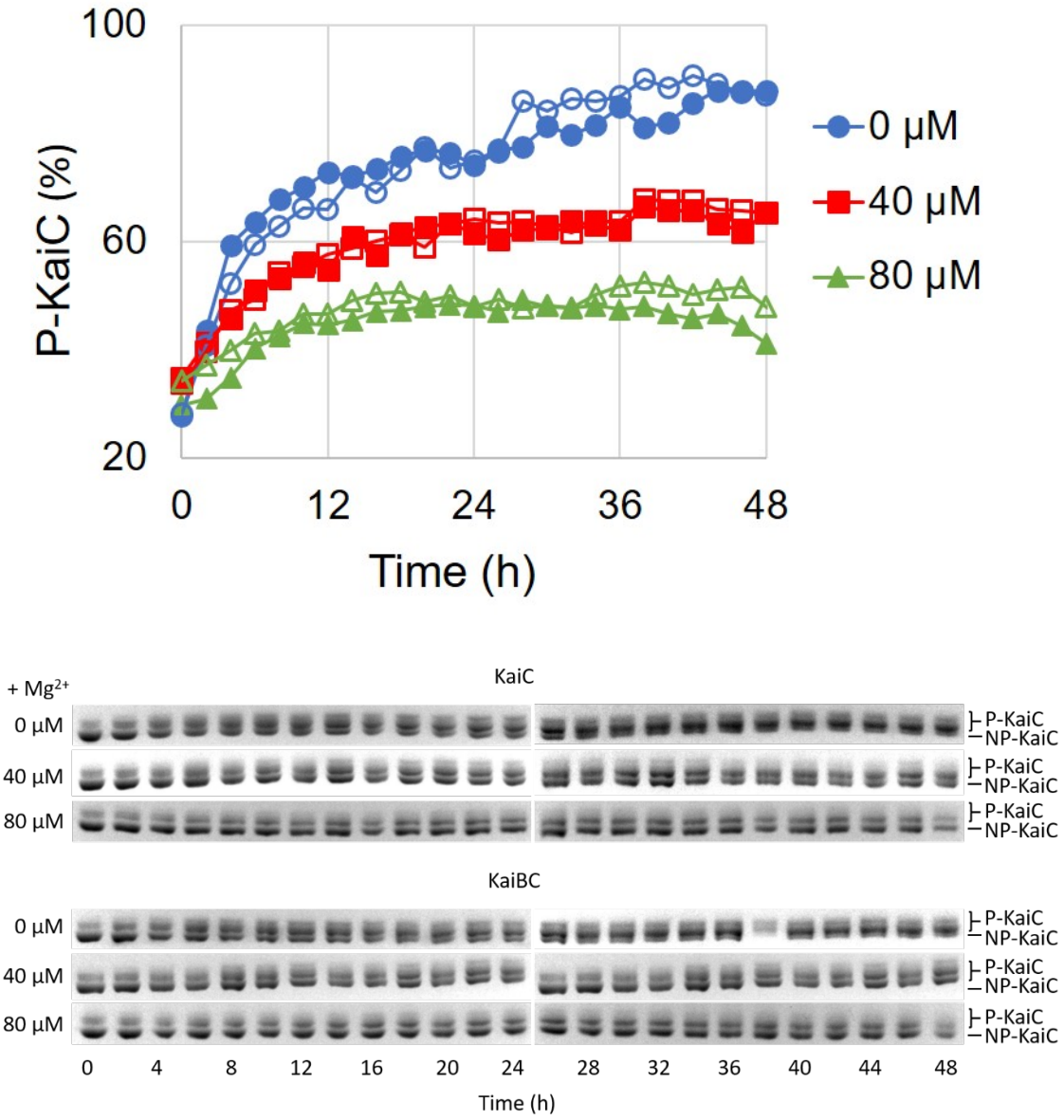

Fig. S11. The phosphorylation state of KaiC.
Time course of phosphorylation of KaiC alone (solid) and KaiBC (open) in various magnesium concentrations.

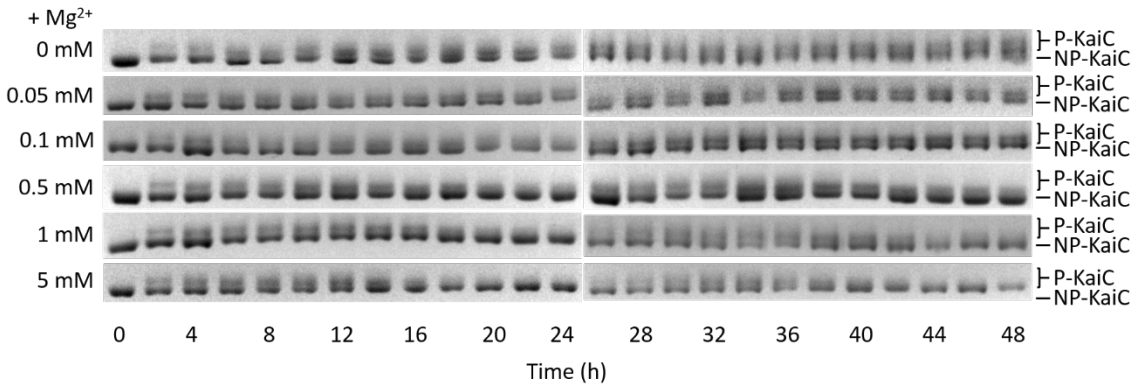

Fig. S12. The phosphorylation state of the hourglass timer of KaiBC.
The densitometry analysis of the bands is shown in Fig.4d.

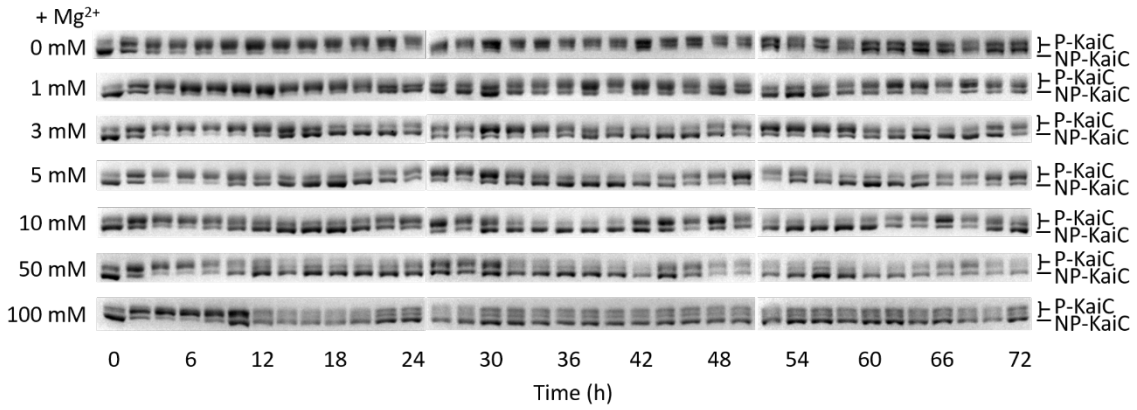

Fig. S13. The phosphorylation state of KaiABC in vitro oscillator.
The densitometry analysis of the bands is shown in Fig.4e.

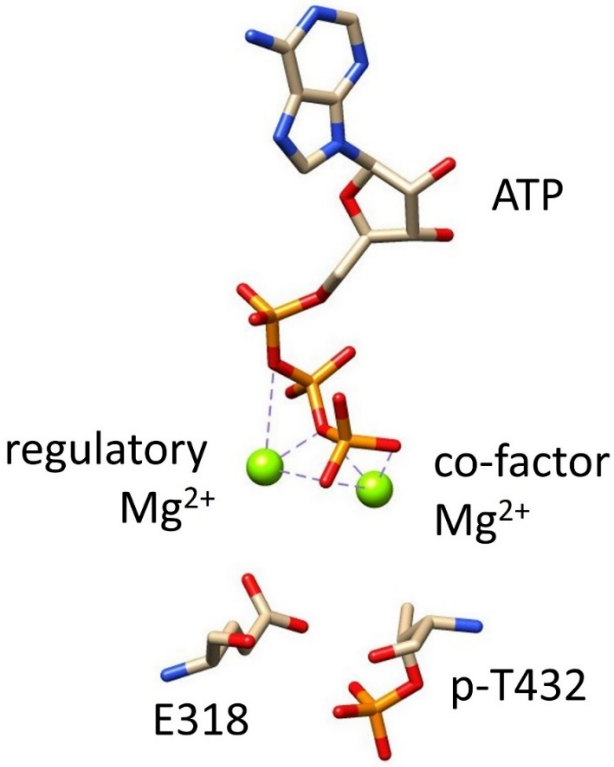

Fig. S14. The active site structures of KaiC S431A mutant (PDB ID: 3k0a).
The structures with two magnesium ions bound can also be found in KaiC S431D (PDB ID: 3k09) and KaiC S431E/T432E (PDB ID: 3s1a).